

An In Vivo Porcine Dataset and Evaluation Methodology to Measure Soft-Body Laparoscopic Liver Registration Accuracy with an Extended Algorithm that Handles Collisions

Richard Modrzejewski · Toby Collins ·
Barbara Seeliger · Adrien Bartoli ·
Alexandre Hostettler · Jacques
Marescaux

Received: date / Accepted: date

Abstract

Purpose The registration of pre-operative 3D images to intra-operative laparoscopic 2D images is one of the main concerns for augmented reality in computer assisted surgery. For laparoscopic liver surgery, while several algorithms have been proposed, there is neither a public dataset nor a systematic evaluation methodology to quantitatively evaluate registration accuracy.

Method Our main contribution is to provide such a dataset with an in vivo porcine model. It is used to evaluate a state-of-the-art registration algorithm that is capable of simultaneous registration and soft-body collision reasoning.

Results The dataset consists of 13 deformed liver states, with corresponding exploration videos and interventional CT acquisitions with 60 small artificial fiducials located on the surface of the liver and distributed within the parenchyma, where a precise registration is crucial for augmented reality. This dataset will be made public. Using this dataset, we show that collision reasoning improves performance of registration for strong deformation and independent lobe motion.

Conclusion This dataset addresses the lack of public datasets in this field. As an example of use, we present and evaluate a state-of-the-art energy based approach and a novel extension that handles self-collisions.

Keywords evaluation dataset · deformable registration · augmented reality

Richard Modrzejewski
EnCoV, Institut Pascal, UMR 6602, CNRS/UBP/SIGMA, 63000 Clermont-Ferrand
E-mail: Richard.MODRZEJEWSKI@uca.fr

Toby Collins
IRCAD and IHU-Strasbourg, 1 Place de l'Hopital, 67000 Strasbourg
E-mail: Toby.COLLINS@ircad.fr

1 Introduction and Background

1.1 Augmented Reality guidance for laparoscopic liver surgery

In laparoscopic liver surgery, the organ is not manipulated directly by hand as in open surgery, where tactile feedback facilitates localization of the substructures by the surgeon. Augmented Reality (AR) can help the surgeon by augmenting the laparoscopic images with pre-operative or intra-operative data such as tumors or vessels, to show their positions below the liver surface. For this purpose, pre-operative 3D images containing segmented substructures have to be registered to the intra-operative laparoscopic 2D images. Because of the insufflation that causes strong deformation of the liver [26], deformable registration has to be used. Moreover, the pre-operative 3D image does not contain texture information to track the model over time, as required in many tracking systems [6].

The common approach to the AR pipeline is to divide the problem into two steps [13, 7]. First, an initial registration of the pre-operative 3D model to the intra-operative 2D images is computed. The 2D images are extracted from an exploration video, where the deformation is assumed constant. This video is captured at the early stage of the surgery where the surgeon records as much of the liver surface as possible. The registration uses geometric cues only during this step. Once this initial registration is performed, the model can be textured and texture-based tracking used for the rest of the intervention.

1.2 Limitations of existing registration solutions

The registration of intra-operative CT images to laparoscopic 2D images of the exploration video is defined as the initial registration problem. In the literature, there are three main approaches to this problem: manual alignment, automatic rigid registration and deformable registration. Manual alignment can be done by a specialist between the 3D pre-operative images and 2D intra-operative images. This solution is relevant only when considering small deformations with almost rigid organs. Moreover, a specialist in anatomy is needed during the procedure, and the result and time needed for the procedure are strongly operator-dependent. If the deformation is negligible, another solution is to search for the rigid transform that minimizes the distance between surface points of the transformed model and the target surface. Concretely, anatomical features can be used to initialize an ICP algorithm [4]. The algorithm may fail if the features used are hardly seen in the 2D images. For strong deformations, deformable registration has to be used. This is technically very challenging and involves organ-specific parameter tuning. There are two main techniques when considering deformable registration in laparoscopic liver surgery. The first one is simulation-based where the liver and all the applied forces are modeled [2]. The main problems of these methods are the need to determine constraints on the model as forces and the fact that it may be slow as it relies

on iterative resolution. The second technique is energy-based. The registration is considered as a minimization problem with a data-association term and a regularization term. The first term represents how the model fits the data and the second term represents how the model is limited in its deformation. There are two types of energy-based method: single image registration and multi-image registration. In single image registration, contours are often used to create the data-association term [1, 18, 14]. In multi-image registration, a surface is reconstructed from the image sequence and the problem is cast as a registration of the surface of the 3D volumetric model to this 3D reconstructed surface [15, 21].

As for the tracking problem, different configurations have been studied in the literature. The first one is to consider deformation but no camera motion [18]. The second one considers only camera motion and no deformation [19]. Both are in general not realistic when considering deformable organs and in vivo data. The last approach considers both camera motion and organ deformation [7] and corresponds to the general context of surgery.

In all these works, registration accuracy is rarely measured and a precise and reliable evaluation is never achieved. Moreover, failures in poorly conditioned cases are neither shown nor discussed. When an in vivo quantitative evaluation is performed, it is done with private data made for the purpose of the experiment. Consequently, the result is never fully reproducible and comparable with the rest of the literature. This problem is caused by a lack of open in vivo datasets for registration evaluation which would be possible to use as a reference. Because of this, it is difficult for these methods to enter clinical trials, through the lack of reliable proofs of their accuracy. Another issue is the fact that these methods are limited to controlled manipulation (resection is forbidden) and there is no reasoning about external and self-collisions, whereas collision can add valuable constraints and can prevent some non-plausible registration solutions.

1.3 Previous attempts to measure registration accuracy

Measuring registration accuracy is difficult because in practice the ground-truth deformation of real tissues is extremely hard to obtain. In the literature, two quantitative values are often discussed when considering evaluation: Target Registration Error (TRE) and Fiducial Registration Error (FRE). FRE is the error distance between the deformed position of markers that have been used to constrain the registration and their ground-truth position. This can be seen as the residual error of the registration. TRE is the error for points of the model that have not been used to constrain the registration. In ICP-based registration, where fiducials are not used, we can consider that the surface-to-surface error represents the FRE. Nevertheless, when considering deformable registration, the surface-to-surface error does not provide a good metric to evaluate the results. Indeed, as the model can be deformed to fit any surface if flexible enough, there is no warranty concerning the realism of this deforma-

tion. Moreover, the absence of dependency between FRE and TRE has been shown [11,12]. Therefore when considering registration evaluation, TRE has to be preferred in all cases.

In order to evaluate registration algorithms, different approaches have been proposed. The easiest way to obtain quantitative results is to perform the evaluation on simulated *in silico* data [21,18,14]. With such an approach TRE can be computed by adding virtual markers in the data, and surface-to-surface error is also easy to obtain. Nevertheless, in this case, a physical characterization and simulation of the organ has to be done, which requires simplified modeling and has no guarantee for the realism of the simulation. Other approaches use physical silicon models (phantoms) [25,5,15,16] where only the physical characteristics of the organ have to be determined. Nevertheless, realistic phantoms of the liver are expensive to produce, and it is difficult to replicate *in vivo* conditions.

When it comes to *in vivo* evaluation, qualitative evaluations are often preferred because of the difficulty to obtain ground-truth for this configuration. Attempts have been made by [24] to obtain quantitative error evaluation for *in vivo* data by evaluating the reprojection error of detected features located on the liver surface. But in contrast to TRE, the error obtained is highly dependent on the quality of the marker association in the algorithm. Moreover, only the error on the surface is estimated.

In summary, while *in silico* and phantom datasets for TRE evaluation exist [23], there is no *in vivo* liver data for TRE evaluation to date.

1.4 Contributions

Our first contribution is an *in vivo* dataset (Fig. 1) and evaluation methodology for TRE evaluation using internal and external artificial landmarks (metal spheres and clips). The dataset includes 13 interventional CT images with contrast injection of a pig liver in different deformed states. For each state, there is one exploration video, and a 3D surface reconstruction computed with a state-of-the-art dense SfM method (photoscan). During CT images acquisition and video recording, the breathing was stopped (apnea). Interventional reconstructions were aligned to the corresponding CT image in order to obtain the position of the markers when using the surface reconstruction as target. Clips and spheres were associated using a novel interactive graph-based matching algorithm. The associations allow evaluating TRE at each clip or sphere in all deformation states. The dataset also includes a carefully segmented 3D liver model, with individual lobes segmented. Such a geometry in a liver model has never been achieved before (lobes are always considered fused into one virtual lobe in the model). The problem with fused lobes is that it fundamentally prevents individual lobe motion being recovered. This is the first systematic database to measure quantitative external and internal registration accuracy (TRE) for laparoscopic liver registration. This will be made public and help drive AR research to have better evaluation standardization and transparent,


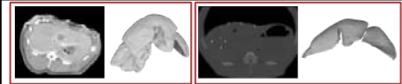
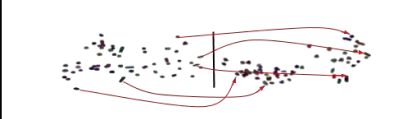
	<ul style="list-style-type: none"> • 13 deformation configurations for the liver and for each of them, an exploration video (~40 s) • For each video, a reconstructed surface built using photoscan-pro
	<ul style="list-style-type: none"> • One pre-operative CT image acquisition and a corresponding 3D geometric model of the liver • 13 intra operative CT image acquisitions with markers localizations and segmented surface
	<ul style="list-style-type: none"> • 13 association files. For all the configurations, all spheres and clips have an association in the reference configuration • Quantification of the deformation using procrustes analysis : after rigid registration, the average residual marker displacement varies from 33 (± 22) mm to 105 (± 60) mm (for a liver size of about 1900 cm³)

Fig. 1 Composition of the proposed dataset.

consistent evaluation. All registration algorithms can be processed and ranked with this dataset based on this error metric. This dataset is used in this paper to evaluate a state-of-the-art initial registration algorithm but can also be used in the future for evaluating registration updating algorithms and evaluating interventional 3D reconstruction accuracy. This is an important and open topic and there exists no public dataset for measuring error in vivo. Many algorithms need training data to extract the parameters they will use. If only few data are needed, one could only use one randomly selected configuration for this and process the error with the entire dataset (we chose this method and used the 8th configuration for our tests). If not, data should be split in training and testing data, and when comparing two algorithms, the same subsets have to be used.

Our second contribution is an adaptation of a state-of-the-art initial registration algorithm to include self-collision constraints. Self-collision constraints are necessary to handle the deformation of non-convex structures, in particular, they are necessary for handling the lobes of the porcine liver. They are also necessary when considering the collision between different organs but this has not yet been attempted in the literature.

2 Evaluation methodology

2.1 Description of the procedure

The method is presented in Fig. 2. The new in vivo evaluation dataset presented was obtained on a 50Kg male Large White Pig (*Sus scrofa domestica*). By laparotomy, the liver surface was exposed. Fifteen metal clips of 1cm length were distributed evenly on the ventral liver surface. Additionally, 45 metal spheres of 2mm diameter were introduced into the liver parenchyma. This was achieved by accessing the dorsal aspect of each liver lobe and the spheres were placed by use of an introduction catheter, in order to avoid surface lesions indicative of their location (1). The laparotomy was then closed and we proceeded to a laparoscopic approach. After trocar placement, the

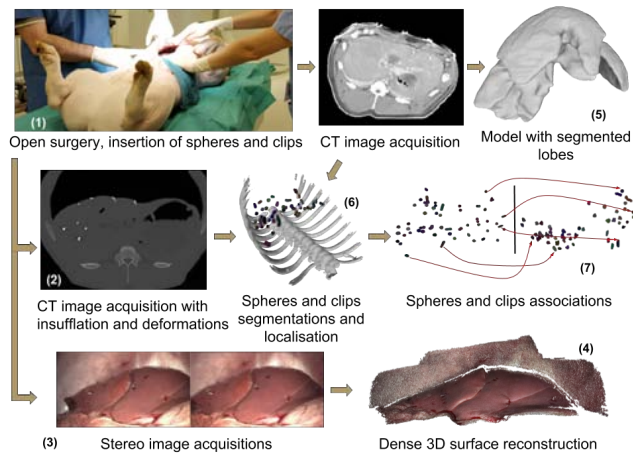


Fig. 2 Evaluation procedure and provided dataset.

abdominal cavity was insufflated with a standard CO₂ pressure (12 mmHg). By moving the four porcine liver lobes into different positions, 13 different laparoscopic configurations were obtained and laparoscopic surface exploration with a 3D camera system (3) was recorded on video for each of them. The datasets were complemented by a computed tomography (CT) scan for each configuration to obtain the position of the markers we use to measure the registration error (2). Two registration targets were considered. The first was to use a segmentation of the surface of the liver using the CT images. This was performed in order to test the registration algorithm reliability in the optimal setting, obtaining a reconstruction of the complete liver surface. In practice, only a portion of the liver surface is reconstructed. The second approach was to use as target a surface reconstruction, built from the video acquired by laparoscopic exploration. It was done using photoscan-pro¹, a state-of-the-art surface reconstruction software (4). When the laparoscopic phase was completed, the laparotomy was re-opened. We additionally separated the four liver lobes by placing interlobar contrast-agent soaked gauze swabs to facilitate discrimination of lobar margins on the subsequent CT scan. This CT scan served to clearly identify the lobe boundaries and was used to build our reference model with segmented lobes (5). At the end of the procedure, the pig was humanely sacrificed according to the protocol.

2.2 Position and correspondences of the markers between views

From the CT images obtained, we segmented the metal markers and classified them as sphere or clip depending on their shape (6). We performed rigid

¹ <http://www.agisoft.com>

registration of the reconstructed surface to the surfaces extracted from CT images using ICP in order to work only in the CT world coordinate system. The only remaining work was to associate all the markers with each other for the different configurations (7) in order to allow TRE computation. Indeed, once this is done, the interpolated positions of each marker can be compared to the position of their association in reference configuration: the ground-truth. The association problem was set as a graph matching problem. For each marker, we searched an association with another marker of the same class (sphere or clip) and that preserves the neighbourhood: the difference of distances between the marker and one of its neighbours in the initial configuration and in the deformed configuration should be minimal. We searched associations that minimize the sum of all these differences. Nevertheless, this problem is NP hard. In order to overcome this, we set the problem as a graph matching problem as proposed in [9]. This is illustrated in Fig. 3. Each node represents an association. In the example provided, $A_{i,j}$ represents the association of the marker i in the reference position and j in the deformed position. E_{ij-kl} represents the probability or likelihood to accept the next association in the graph $A_{k,l}$ by considering the previous association $A_{i,j}$ as true. We do not consider nodes representing associations between spheres and clips. We do neither consider arcs that allow to re-associate the same marker. For instance, there is no arc between $A_{2,2}$ and $A_{3,2}$ (because it would associate the marker number 2 twice). We also do not consider arcs which consider an association where the reference point is not in the neighbourhood of the previous point. We set:

$$E_{ij-kl} = \exp(-\lambda|\text{dist}(\text{Ref}_i, \text{Ref}_k) - \text{dist}(\text{Def}_j, \text{Def}_l)|) \quad (1)$$

where Ref_i and Ref_j are the centroids of the markers i and j in the reference position and Def_k and Def_l are the positions of the markers k and l in deformed position. Nevertheless, because of the fact that the markers are not densely present everywhere in the liver and because of strong deformations, the exact solution of this problem may not coincide with the real markers association when considering these constraints only. In order to overcome this, we added extra constraints to this problem by manually fixing some associations (corresponding to removing nodes in the graph). We built up an interface which allows us to refine iteratively the solution provided by the graph matching optimization, by adding extra constraints by manually clicking the corrected associations and achieve correct associations. From a marker in the reference view and the result of the registration for one deformation, one can interpolate the position of this marker after deformation and compare it to the associated marker in the ground-truth.

3 Registration Methodology

The deformable registration algorithm presented here is based on previous work [20,7,3] where the problem is formulated as an iterative energy minimization. As a target for the registration, we consider multi-image registra-

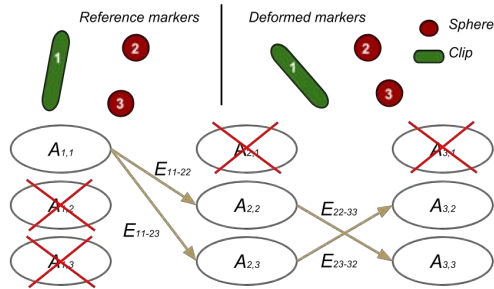


Fig. 3 Graph formulation of the association problem using 3 markers.

tion: not only one image is used, but a surface of the liver reconstructed from an exploration video is used as 3D target surface.

3.1 Terms definition and registration approach

In order to properly segment the different lobes of the liver, recall that they were wrapped in tissues with contrast agent before the reference CT. Doing that, the boundary between the lobes was reinforced in the images and semi-automatic segmentation was much easier to perform. From this extracted surface, we used Tetgen² to generate the tetrahedral mesh from surface triangles. We take as input a bio-mechanical model representing the pre-operative liver generated using the tetrahedral mesh. We denote the model's surface vertices as \mathcal{V}_s . We use $f(\mathbf{p}; \mathbf{x}) : \mathbb{R}^3 \rightarrow \mathbb{R}^3$ to denote the transform of a 3D point \mathbf{p} in the initial configuration to the surface reconstruction coordinates. This is parametrized by an unknown vector \mathbf{x} , and the task is to recover it. From this exploration video, we use the associated surface reconstruction as the target of the registration. The vertices of this surface are denoted \mathcal{Q} . Without considering the collisions, the problem to minimize is :

$$E_0(\mathbf{x}) = E_M(\mathbf{x}) + \lambda_{ICP} E_{ICP}(\mathbf{x}; \mathcal{V}_s, \mathcal{Q}) + \lambda_{cont} E_{3Dcontours}(\mathbf{x}, \mathcal{Q}), \quad (2)$$

where $\lambda_{ICP} \in \mathbb{R}^+$, and $\lambda_{cont} \in \mathbb{R}^+$ are respectively the ICP weight and the contours weight (in our tests we use $\lambda_{ICP} = 6.1$ and $\lambda_{cont} = 100.0$). The term E_M represents the mechanical energy of the system. In our experiments we use a mass spring model energy but any other model can be used. In our experiments we model $E_M(\mathbf{x})$ using a mass-spring model generated from a tetrahedral mesh of our reference liver. The term E_{ICP} is the *deformable ICP energy*, which attracts the model's transformed surface vertices \mathcal{V}_s to fit their closest vertices in \mathcal{Q} . It constrains the model to fit the target surface. In order to overcome convergence issues associated with point-to-point ICP, we use point-to-plane ICP instead that allows the surfaces to slide across one another

² <http://wias-berlin.de/software/tetgen>

during registration. $E_{3Dcontours}(\mathbf{x}, \mathcal{Q})$ is the contour energy, that helps the registration by using fixed position constraints. 3D landmarks located on the contours of the lobes are localized in the model and in the target. In this work, these are selected manually but it would be possible to automatize this step in future works. All these terms are explained in [20]. We propose to complete this energy with a term to prevent self collision, as:

$$E(\mathbf{x}) = E_0(\mathbf{x}) + \lambda_{col} E_{collision}(\mathbf{x}). \quad (3)$$

3.2 Collision model

Collision detection for deformable meshes has received a significant attention in the literature. As direct intersection checking is computationally expensive, most works focus on ways to reduce the search space. In our case, even if the initial registration problem does not have to be solved in real-time, it is still important to reduce the computation time as much as possible.

A first approach is to perform spatial hashing of the object and to use an adaptive bounding box [17]. However, as the mesh is not rigid, the structure of the bounding box has to be recomputed at each step of the registration algorithm and this is hardly parallelizable. As a consequence, this method can massively slow down the registration algorithm. Another approach is to subdivide the space containing the object [22]. The problem is parallelizable but the issue is to define the boundary and the size of the voxels of the grid. This solution can be memory-consuming for large meshes.

In our approach, we propose an intermediate parallel solution. First, we only consider the tetrahedra with at least one face belonging to the surface of the model. Indeed, if self-collision happens in the volume then there is necessarily an intersection somewhere on the surface. Removing these collisions will iteratively remove all the collisions inside the mesh. Once this is done, we consider a GPU thread per tetrahedron. When a collision test is performed, all the threads compute the center and the radius of the circumsphere of their associated tetrahedron. Each thread then tests the intersection between its associated circumsphere and all the others. This test is a simple distance comparison and is not computationally expensive. As each thread runs in parallel, the computation time to take into account is the one of the slowest thread, so there is no need to reduce the number of comparisons here. If a possible collision is detected, then a test is performed by the concerning thread, between the related tetrahedra using [10]. In this method, the search space is reduced by using the spheres, the structure of the model is fast to update, and the memory usage is low and constant. We implemented this collision method on the GPU and tested it with meshes of 68123 tetrahedra on a GeForce GTX 1080. The average time for the collision test is 65 ms.

3.3 Collision energy formulation

Using collision detection, we defined $E_{collision}$ as the self-collision energy term in the registration energy, which allows the model to recover as soon as a self-collision is detected on the surface of the mesh. This energy is defined as:

$$E_{collision}(\mathbf{x}; \mathcal{V}_s, Q) = \sum_{collisions} \|x_c - (x_{ci} + \mu_{sharpness} n_{surface})\|^2, \quad (4)$$

where x_c are the points of the colliding tetrahedron, x_{ci} is the position of the colliding point in the previous step, $\mu_{sharpness}$ (set as 0.01 in our experiments) is a weight controlling the rectification step and $n_{surface}$ is the normal in x_{ci} . Contrary to [20], the collision energy is only a rectification term that works iteratively. The final solution is an equilibrium where there are small oscillations around small surface collisions (there is no energy preventing future collision). A global energy collision term would require computing the relative distance field to the mesh surface but this is computationally expensive. Our solution is an alternative where real-time processing is still available.

3.4 Resolution of the minimisation problem

In order to reduce computation time, we use the method in [7] to reduce the deformable model’s deformation space, exploiting the fact that feasible deformations tend to be mostly smooth. We optimize $E(\mathbf{x})$ iteratively using a stiff-to-flexible strategy [8,3], which is important to avoid local minima. Initially the model is kept rigid, by setting λ_{ICP} to a small value. We then optimize $E(\mathbf{x})$ using a single Gauss-Newton iteration, and increase λ_{ICP} by a factor. λ_{cont} and λ_{col} (set as 100 in our experiments) are kept fixed. We then repeat the process, truncating λ_{ICP} to a maximal value, which we set to 10 times the initial value. We continue until convergence is detected or a maximum number of iterations is reached. We initialize using a manual roughly-estimated rigid transform.

4 Experimental Results

We used the dataset presented in section 2 to evaluate the registration algorithm. In order to evaluate the benefit of using segmented lobes and collision constraints, we tested two configurations for the model using the previously described dataset. The first set of tests (Fig. 4) was done with a model where lobes are fused together. This correspond to the human case but this is not very accurate here because of the sliding between lobes we have for some deformations. The second one (Fig. 5) was performed on a model where the lobes are segmented. In the second set of tests, we tested our registration with (a) and without (b) collision constraints. For both tests, we did two evaluations. One where the TRE of all the markers are considered (a and b). This allows

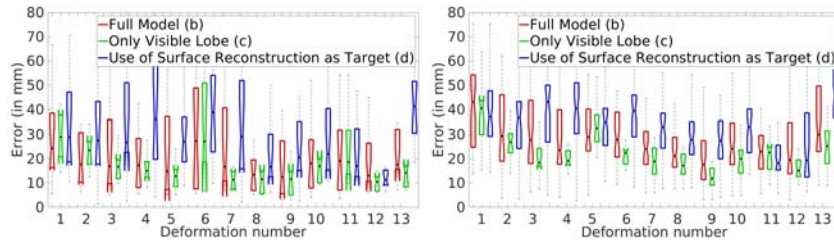


Fig. 4 Registration errors on the surface (left) and inside the liver (right) when considering a non segmented lobes model. (b,c,d) are explained in section 4.

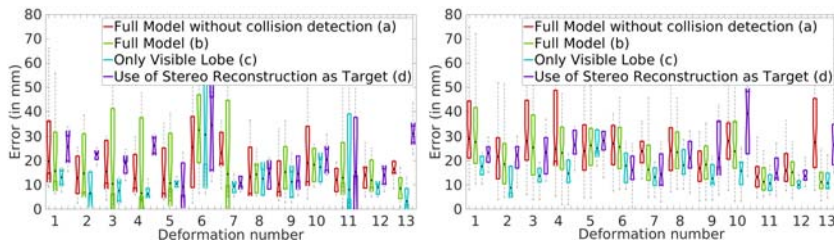


Fig. 5 Registration errors on the surface (left) and inside the liver (right) when considering a model where lobes are segmented. (a,b,c,d) are explained in section 4.

us to evaluate the registration on the whole model and see the effects of lobes interacting with each other. The other one only considers the markers of the visible lobe (c and d) where the target surface is properly reconstructed. These are the results we should look at when evaluating the precision, as in practice, during a surgery, the surgeon visualizes only the relevant liver lobe. We performed the evaluation tests using the segmented surface from the CT as a target (a, b and c) and also the reconstructed surface built from the exploration video (d). The first test evaluates the results we would obtain if our reconstructed surfaces were perfect. The second test evaluates the registration in real conditions (noise in the reconstruction, missing parts). This separation allows us to decouple registration error caused by an incomplete interventional reconstruction and error caused by the registration algorithm.

Qualitatively, we see in Fig. 6 that after registration, the collision cost behaves as expected: without it, we see deep collision between lobes but with it, only small residual collisions remain. The quantitative results are shown in Fig. 4 and Fig. 5. Results are in general slightly better when using the model with segmented lobes ($\simeq 10$ mm improvement for the inside and $\simeq 5$ mm for the surface). Concerning the error inside the liver, the collision constraints improve the quality of the registration ($\simeq 1$ - 2 mm of improvement). This demonstrates the benefit of such an approach. When considering only the spheres and clips of the visible lobe, and using the model where collision is taken into account, the median error is around 20 mm inside the liver and 15 mm at the surface.

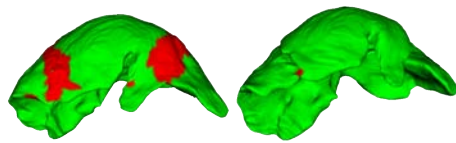


Fig. 6 Deformed mesh after registration without (left) and with (right) collision constraints. In red are the collision areas.

5 Conclusion

We have presented a new in vivo porcine liver registration evaluation dataset that addresses the lack of public datasets in this field, as it will be made public. TRE can be evaluated on the surface and within the liver. Surface-to-surface error can also be computed using the segmented CT images, but as a way to check the behavior and convergence of the algorithms and not as an evaluation metric. This dataset is the very first of its kind. As an example of use, we have presented and evaluated a state-of-the-art energy based approach and a novel extension that handles self-collisions. This can be extended straightforwardly to handle collisions with other surrounding organs or instruments.

6 Compliance with Ethical Standards

The authors declare that they have no conflict of interest. All applicable international, national, and institutional guidelines for the care and use of animals were followed. All procedures performed in studies involving animals were in accordance with the ethical standards of the institution at which the studies were conducted.

References

1. Adagolodjo, Y., Trivisonne, R., Haouchine, N., Cotin, S., Courtecuisse, H.: Silhouette-based pose estimation for deformable organs application to surgical augmented reality. In: *Intelligent Robots and Systems (IROS)*, pp. 539–544. IEEE (2017)
2. Allard, J., Cotin, S., Faure, F., Bensoussan, P.J., Poyer, F., Duriez, C., Delingette, H., Grisoni, L.: Sofa-an open source framework for medical simulation. In: *MMVR 15-Medicine Meets Virtual Reality*, vol. 125, pp. 13–18. IOP Press (2007)
3. Amberg, B., Romdhani, S., Vetter, T.: Optimal step nonrigid icp algorithms for surface registration. In: *CVPR'07. IEEE Conference on*, pp. 1–8. IEEE (2007)
4. Clements, L.W., Chapman, W.C., Dawant, B.M., Galloway Jr, R.L., Miga, M.I.: Robust surface registration using salient anatomical features for image-guided liver surgery: Algorithm and validation. *Medical physics* **35**(6Part1), 2528–2540 (2008)
5. Collins, J.A., Weis, J.A., Heiselman, J.S., Clements, L.W., Simpson, A.L., Jarnagin, W.R., Miga, M.I.: Improving registration robustness for image-guided liver surgery in a novel human-to-phantom data framework. *IEEE transactions on medical imaging* **36**(7), 1502–1510 (2017)
6. Collins, T., Bartoli, A.: [poster] realtime shape-from-template: System and applications. In: *ISMAR, 2015 IEEE International Symposium on*, pp. 116–119. IEEE (2015)

7. Collins, T., Bartoli, A., Bourdel, N., Canis, M.: Robust, real-time, dense and deformable 3d organ tracking in laparoscopic videos. In: MICCAI, pp. 404–412. Springer (2016)
8. Collins, T., Chauvet, P., Debize, C., Pizarro, D., Bartoli, A., Canis, M., Bourdel, N.: A system for augmented reality guided laparoscopic tumour resection with quantitative ex-vivo user evaluation. In: CARE, pp. 114–126. Springer (2016)
9. Cour, T., Srinivasan, P., Shi, J.: Balanced graph matching. In: Advances in Neural Information Processing Systems, pp. 313–320 (2007)
10. Eberly, D.: Intersection of convex objects: The method of separating axes. Geometric Tools, LLC <http://www.geometrictools.com>,(1998- 2008) (2001)
11. Fabian, S., Spinczyk, D.: Target registration error minimization for minimally invasive interventions involving deformable organs. *Computerized Medical Imaging and Graphics* **65**, 4–10 (2018)
12. Fitzpatrick, J.M.: Fiducial registration error and target registration error are uncorrelated. In: Medical Imaging 2009: Visualization, Image-Guided Procedures, and Modeling, vol. 7261, p. 726102. International Society for Optics and Photonics (2009)
13. Haouchine, N., Dequidt, J., Peterlik, I., Kerrien, E., Berger, M.O., Cotin, S.: Image-guided simulation of heterogeneous tissue deformation for augmented reality during hepatic surgery. In: ISMAR, 2013 IEEE International Symposium on. IEEE (2013)
14. Haouchine, N., Roy, F., Untereiner, L., Cotin, S.: Using contours as boundary conditions for elastic registration during minimally invasive hepatic surgery. In: Intelligent Robots and Systems (IROS), 2016 IEEE/RSJ International Conference on. IEEE (2016)
15. Heiselman, J.S., Collins, J.A., Clements, L.W., Weis, J.A., Simpson, A.L., Geevarghese, S.K., Kingham, T.P., Jarnagin, W.R., Miga, M.I.: Nonrigid registration for laparoscopic liver surgery using sparse intraoperative data. In: Medical Imaging 2018: Image-Guided Procedures, Robotic Interventions, and Modeling, vol. 10576, p. 105760D. International Society for Optics and Photonics (2018)
16. Kerdok, A.E., Cotin, S.M., Ottensmeyer, M.P., Galea, A.M., Howe, R.D., Dawson, S.L.: Truth cube: Establishing physical standards for soft tissue simulation. *Medical Image Analysis* **7**(3), 283–291 (2003)
17. Klosowski, J.T., Held, M., Mitchell, J.S., Sowizral, H., Zikan, K.: Efficient collision detection using bounding volume hierarchies of k-dops. *IEEE TVCG* pp. 21–36 (1998)
18. Koo, B., Özgür, E., Le Roy, B., Buc, E., Bartoli, A.: Deformable registration of a preoperative 3d liver volume to a laparoscopy image using contour and shading cues. In: MICCAI, pp. 326–334. Springer (2017)
19. Mahmoud, N., Cirauqui, I., Hostettler, A., Doignon, C., Soler, L., Marescaux, J., Montiel, J.: Orbslam-based endoscope tracking and 3d reconstruction. In: CARE, pp. 72–83. Springer (2016)
20. Modrzejewski, R., Collins, T., Bartoli, A., Hostettler, A., Marescaux, J.: Soft-body registration of pre-operative 3d models to intra-operative rgbd partial body scans. In: MICCAI, pp. 39–46. Springer (2018)
21. Plantefeve, R., Peterlik, I., Haouchine, N., Cotin, S.: Patient-specific biomechanical modeling for guidance during minimally-invasive hepatic surgery. *Annals of biomedical engineering* **44**(1), 139–153 (2016)
22. Rumman, N.A., Schaerf, M., Bechmann, D.: Collision detection for articulated deformable characters. In: Proceedings of the 8th ACM SIGGRAPH Conference on Motion in Games, pp. 215–220. ACM (2015)
23. Suwelack, S., Röhl, S., Bodenstedt, S., Reichard, D., Dillmann, R., Santos, T., Maier-Hein, L., Wagner, M., Wünscher, J., Kennigott, H.: Physics-based shape matching for intraoperative image guidance. *Medical physics* **41**(11) (2014)
24. Thompson, S., Schneider, C., Bosi, M., Gurusamy, K., Ourselin, S., Davidson, B., Hawkes, D., Clarkson, M.J.: In vivo estimation of target registration errors during augmented reality laparoscopic surgery. *CARS* **13**(6), 865–874 (2018)
25. Thompson, S., Totz, J., Song, Y., Johnsen, S., Stoyanov, D., Ourselin, S., Gurusamy, K., Schneider, C., Davidson, B., Hawkes, D.: Accuracy validation of an image guided laparoscopy system for liver resection. In: Medical Imaging 2015: Image-Guided Procedures, Robotic Interventions, and Modeling, vol. 9415, p. 941509. SPIE (2015)
26. Zijlmans, M., Langø, T., Hofstad, E.F., Van Swol, C.F., Rethy, A.: Navigated laparoscopy–liver shift and deformation due to pneumoperitoneum in an animal model. *Minimally Invasive Therapy & Allied Technologies* **21**(3), 241–248 (2012)